# Characterization and Evaluation of Carboxymethyl Cellulose-Based Films for Healing of Full-Thickness Wounds in Normal and Diabetic Rats

Poulami Basu,[†] Uttamchand Narendrakumar,[‡] Ruckmani Arunachalam,[§] Sobita Devi,[§] and Inderchand Manjubala*,[†]

[†]Department of Bio Sciences, School of Bio Sciences and Technology, and [‡]Department of Manufacturing, School of Mechanical Engineering, Vellore Institute of Technology, Vellore 632014, India

[§]Department of Pharmacology, Chettinad Hospital and Research Institute, Chettinad Academy of Research and Education, Chennai 603103, India

ABSTRACT: Artificial skin substitute made of polymeric films are of great demand in the field of skin tissue engineering. We report here the fabrication of carboxymethyl cellulose (CMC) and poly(ethylene glycol) (PEG) blend films by solution casting method for wound healing applications. The physicochemical characteristics and the thermal stability of the films were analyzed. The surface morphology shows crystalline structures with large hexagonal-like platelet crystals of CMC on the surface of the films. Pure CMC films exhibited higher tensile strength than the CMC/ PEG blend films. The swelling ratio (SR) of the films was influenced by the pH of Tris−HCL buffer (2.0, 5.0, and 7.0), which increased with increase in pH. The hemocompatibility assay and cytotoxicity test using NIH 3T3 fibroblast cells showed that the films were biocompatible. To evaluate the wound healing efficacy, the films were applied in full-thickness wounds created in normal and diabetic Wistar albino rats. The wounds healed faster with pure CMC film compared to blend films in both normal and diabetic rats, evidenced by intensive collagen formation in histopathological analysis. Thus, the films have potential application in skin regeneration, thereby to restore the structural and functional characteristics of the skin.
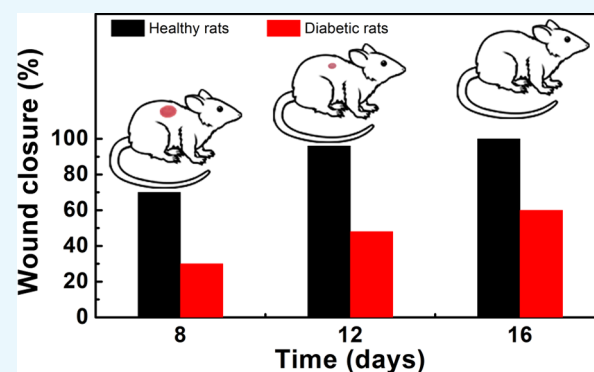
INTRODUCTION

Over the past few decades, a large number of studies have been carried out on various strategies to develop appropriate wound dressing materials to facilitate wound healing by providing template for better recruitment of cells.[1] An ideal wound dressing material should be biocompatible and create a moist environment at the wound site to prevent wound dehydration. Besides, the material should protect the wound from dust and resist microbial invasion, permit gaseous exchange, and promote epithelialization.[2,3]

The widely explored polymer-based wound dressings are tailored from natural polymers like collagen, chitosan, gelatin, keratin, and silk sericin and synthetic polymers such as poly(vinyl alcohol) (PVA), poly(ethylene glycol) (PEG), poly(lactic acid) (PLA), polycaprolactone (PCL), and silicone in the form of film, foam, hydrogel, nanofiber, woven matrix, etc.[4−6] The most accepted biomaterials for wound healing application are collagen, hyaluronic acid, and chitosan, which are low antigenic, biocompatible, and biodegradable.[7−9] Recent findings show the fabrication of hyaluronic acid-grafted pullulan polymers as films for wound healing applications.[10] Electrospun potato starch-based nanofibrous scaffolds were also prepared and utilized to promote cellular proliferation for dermal wound healing.[11] Currently, polymer surgical dressings as sponges based on chitosan/sodium hyaluronate/resveratrol were tailored to evaluate their regenerative effects in wound healing.[12] Besides, the chitosan/collagen/alginate composite was fabricated and evaluated for determining its promoting effect on wound healing.[13] But the use of these polymeric dressing materials is usually limited due to weak mechanical properties, poor biostability, and low shelf life.[14] They have the tendency to shrink, deform, or contract, indicating lack of support for cell ingrowth due to improper maintenance of these materials structures.[15] Gelatin and keratin are used for the fabrication of wound dressings as they have low antigenicity and can promote adhesion, differentiation, and proliferation of cells. Nonwoven wound dressings were fabricated from chicken feather keratin, keratin/chitosan, and keratin/sodium alginate blends for skin regeneration purposes.[16] But the major drawback of the polymers involved is
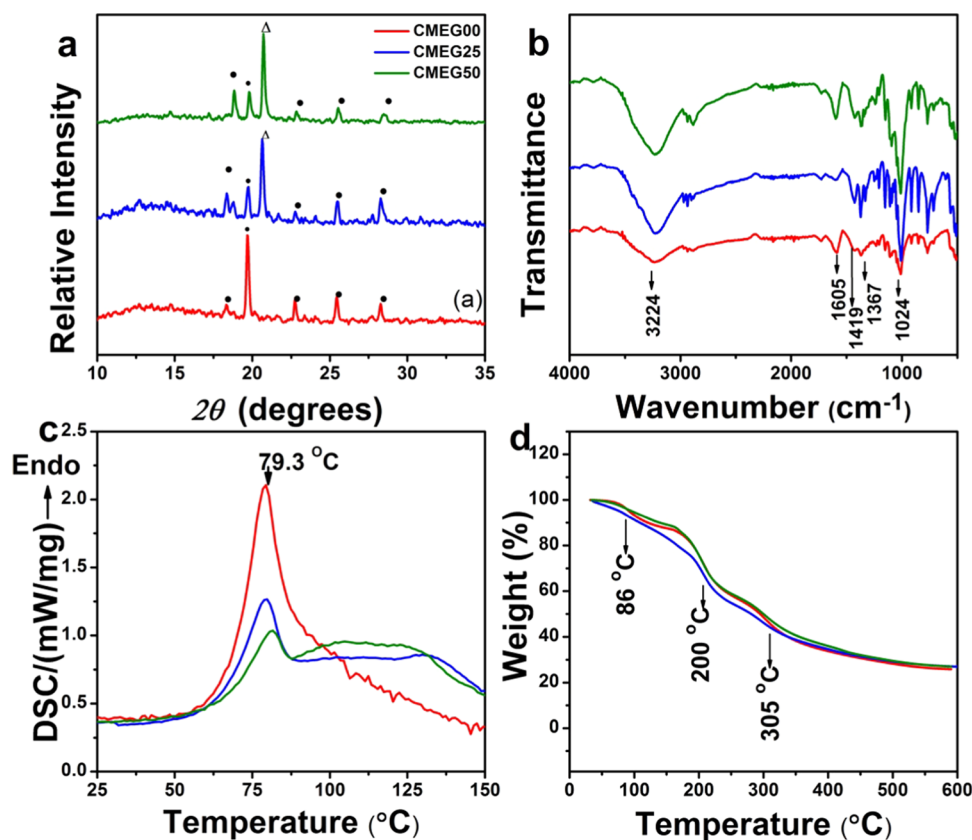
Figure 1. (a) X-ray diffraction patterns of the films. CMC and PEG peaks are indexed as (●) and (Δ), respectively. (b) Fourier transform infrared (FTIR) spectra; (c) differential scanning calorimeter (DSC) curves; and (d) thermogravimetric analyzer (TGA) traces of the films.

their brittleness.[17−19] Silk sericin is also considered as an attractive biomaterial for wound healing owing to its low antigenicity and good mechanical properties.[20] However, sericin sometimes leads to in vivo inflammation as it suppresses proinflammatory cytokines production; hence, the silk is often degummed during silk processing.[21,22] On the other hand, synthetic polymers like PVA, PEG, PLA, PCL, and silicone exhibit appreciable mechanical properties and also diverse plasticity. Insulin delivering nanoparticles of chitosan was embedded on electrospun PCL/collagen matrix to develop potential cutaneous wound care materials.[23] PVA/chitosan/ zinc oxide beads were also investigated as potential elements for wound healing applications.[24] But, synthetic polymers when used alone exhibit immunogenic properties and are lightly toxic in nature. Polyurethane-based commercial wound dressings like Opsite, Tegaderm, and Biooclusive have been marketed, but they possess poor absorbent properties.[25] Lack of biological cues in terms of cellular attachment hinders the use of these synthetic polymers for skin regeneration applications.[19,26] The current strategies focus on the fabrication of wound dressing materials from a new class of polymer and their role in accelerating chronic wound repair by regulated deposition of extracellular matrix.[27]

Carboxymethyl cellulose (CMC), a derivative of cellulose, has been widely used in pharmaceutical industry as emulsifier, viscosity modifier, lubricant, and stabilizer to develop different pharmaceutical dosage formulations.[28,29] CMC is a seminatural polymer and has excellent water-absorbing and swelling capacities.[30] It is physiologically nontoxic and is compatible with mucous membrane, bone, and skin.[31−33] CMC may be used as a template for wound healing and skin regeneration

applications, and there is not much evidence that elaborates on the application of CMC films to treat full-thickness wound or chronic wounds like diabetic foot ulcers. The advantage of CMC is film formulation and the ability to blend with other polymers such as poly(ethylene glycol) (PEG), which is biocompatible, less toxic, and hydrophilic.[34]

The present study aims to fabricate CMC/PEG blend films as wound dressing materials for full-thickness normal and chronic (diabetic) wound healing. As there has been limited reports on the effect of CMC on full-thickness diabetic wound healing process, this work highlights the potential of CMC polymer application in such cases. The films were prepared using solution-casting method and characterized in terms of its physicochemical, thermal, and mechanical properties. The pH-responsive swelling behavior of CMC films in physiological body fluid was also examined. The hemolytic potential and the cytocompatibility of the films were also studied with fibroblast cells. Besides, the novelty of the work lies in utilizing CMC-based films to treat chronic diabetic wounds. A full-thickness wound model was adopted in normal and diabetic rats to study the efficiency of the films for wound closure and skin regeneration.

■ RESULTS

Physicochemical Characterization. The X-ray diffraction (XRD) patterns of the films are shown in Figure 1a. The crystalline nature of CMC is evident with a high intensity peak at 2θ of 19.7°. The other diffraction peaks of CMC are observed at 18.4, 22.7, 25.3, and 28.4°. The peak intensity decreased as PEG concentration increases. This might be due to the hydrogen-bond interaction between the carboxylic

group of CMC and the hydroxyl group of PEG, which resulted in change in the crystallographic position of the two polymers after blending.[35] Only one peak of PEG was observed at 2θ of 20.7°, and other peaks of PEG are not visible due to low concentration of PEG being used in the blend films.

The FTIR spectra of the films are shown in Figure 1b. The band at 1024 cm^{-1} is due to −CH−O−CH$_2$ stretching, and the band at 1419 cm^{-1} is assigned to −CH$_2$ scissoring vibration, whereas the absorption band at 1605 cm^{-1} confirmed the presence of the COO$^-$ group in CMC. The absorption band at 3224 cm^{-1} is attributed to the stretching of the −OH group of CMC. The band at 1150 cm^{-1} is attributed to the stretching of the C−O−C group for PEG. The scissoring and bending of the C−H group for PEG are obtained at 1367 and 1429 cm^{-1}, respectively, and the band at 2892 cm^{-1} is assigned to the stretching of the C−H group. For the blend films, addition of PEG did not influence the structure of CMC.

The thermal behavior of the films analyzed by DSC and TGA is shown in Figure 1c,d. The pure CMC films (CMEG00) have a relatively large sharp endothermic peak at 79 °C, the glass-transition temperature of CMC. A relatively smaller endothermic glass-transition peak for CMEG25 and CMEG50 is observed at 79 and 80 °C, respectively. The addition of PEG in CMC showed a slight variation in the melting temperature, due to the interaction between the functional groups of CMC and PEG. Due to the high hydrophilicity of CMC, it still contained a small amount of moisture water molecules, which is evident from the TGA curve as weight loss (approximately 6%) at 86 °C. The weight loss at 200 °C is due to the removal of carbon dioxide from the polysaccharide chain and degradation of saccharide ring of CMC. The weight loss at 305 °C is attributed due to the breaking of −C−O−C bonds present in CMC.[36,37] The weight losses of the films at 200 and 305 °C are 32 and 55%, respectively. The overall weight loss of the films upon heating to 600 °C is 73%. All of the films degraded effectively on heating, and the presence of PEG in CMC has shown no influence on the thermal property of CMC.

Tensile Properties. The stress vs strain curves of the films are shown in Figure 2. The maximum tensile stress, strength, and Young's modulus were calculated from the stress−strain curves and are tabulated in Table 1. The maximum tensile stress of CMEG00 is 14 ± 3 kPa, higher than that of CMEG25 (8 ± 2 kPa) and CMEG50 (10 ± 3 kPa). The tensile strengths

of CMEG00, CMEG25, and CMEG50 are 13 ± 3, 8 ± 3, and 11 ± 3 kPa, and Young's moduli are found to be 1 ± 0.21, 0.81 ± 0.18, and 1 ± 0.10 kPa, respectively. The films were soft, and the pure CMC films possess better tensile properties than the blend films.

Surface Morphology of the Films. The scanning electron microscopy (SEM) images of the films are shown in Figure 3a−c, The surface shows platelet-like crystallites that are randomly arranged and overlayed on the surface. The crystals seem to be thinner and more concentrated in CMEG25, whereas higher the PEG amount, bigger and more coarse are the crystals.

Effect of pH on Swelling of Films. Water binding and absorption ability of the films are crucial parameters for wound healing. The effect of pH on swelling of the films was investigated in acidic and neutral ranges of pH, and the results are shown in Figure 4. Three different pHs (2.0. 5.0, and 6.0) were chosen to determine the pH-responsive behavior of CMC polymer. The swelling ratios of CMEG00, CMEG25, and CMEG50 in Tris−HCL buffer of pH 2.0 were 1228 ± 34, 1186 ± 32, and 703 ± 56%, respectively, and 1346 ± 32, 1263 ± 58, and 611 ± 42%, respectively, at pH 5.0. The film showed the highest swelling ratios in Tris−HCL buffer at pH 7.0 as 1428 ± 56, 1335 ± 24, and 1190 ± 32% for CMEG00, CMEG25, and CMEG50, respectively. The swelling ratios of CMEG00 and CMEG25 have similar behaviors at all pHs, while CMEG50 showed lower swelling ratios at pHs 2 and 5 and a similar behavior at pH 7. There is a slight decrease of swelling ratio at all pHs with increasing PEG content, but it was not significant. The addition of PEG does not influence the swelling property of CMC.

Biological Characterization. *Hemocompatibility Study.* Hemocompatibility is a key issue for the safety of dressing materials in wound healing. This study reflected the degree of interaction between the films and the blood. The impact of the films via contact activation has been studied. The amount of RBC, WBC, and platelets adhered to the films, percentage hemolysis, and plasma hemoglobin were measured and are summarized in Table 2. The WBC count (%) for the films was found to be higher than the control. On the other hand, it is interesting to see that the RBC and platelet counts (%) for CMEG00 and CMEG25 decreased compared to the control, whereas the values increased for CMEG50. Hemolysis results indicate any undesirable conditions originated from the biomaterials, and a value of 0.2 indicates excellent biomaterial property of pure CMC films.

The SEM images in Figure 5 show the adhered red blood cells on the surface of the films after blood contact, thus indicating the ability of the polymer matrix to entrap blood cells when exposed to blood. The cells are flat and adherent, arranged in layers, and no rupture of the cells was visible in CMEG00. There is a slight fusion or surface destruction in very few cells in CMEG25, while the cells are not as flat as in CMEG50, more or less spherical, and are not arranged very close to each other. This suggests that CMEG00 has the ability to maintain the cell behavior and structure, while in contact with blood, compared to blend films.

Cell Cytotoxicity Study. The cytotoxicity of the film extracts was analyzed by treating with the fibroblast cells (NIH 3T3). The viabilities of the cells in contact with CMEG00, CMEG25, and CMEG50 extracts were found to be 92, 90, and 88%, respectively, and 95% for control medium after 3 days of incubation as evaluated by cell viability analyzer. The cell
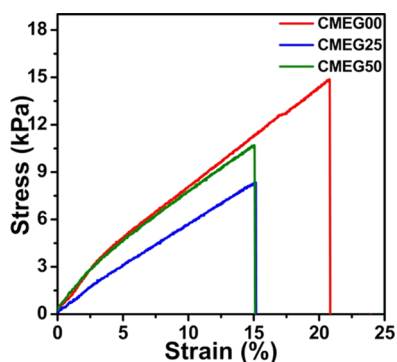

Figure 2. Stress vs strain curves of the films. The maximum tensile stress, ultimate tensile strength, and Young's modulus were calculated from the stress−strain curves.

Table 1. Tensile Properties of the Films in Terms of Maximum Stress, Young's Modulus, and Ultimate Tensile Strength are Determined at Room Temperature by Tensile Test ($n = 6$)

sample id	maximum stress (kPa)	Young's modulus (kPa)	ultimate tensile strength (kPa)
CMEG00	14 ± 3	1 ± 0.2	13 ± 3
CMEG25	8 ± 2	0.81 ± 0.2	8 ± 3
CMEG50	10 ± 3	1 ± 0.1	11 ± 3
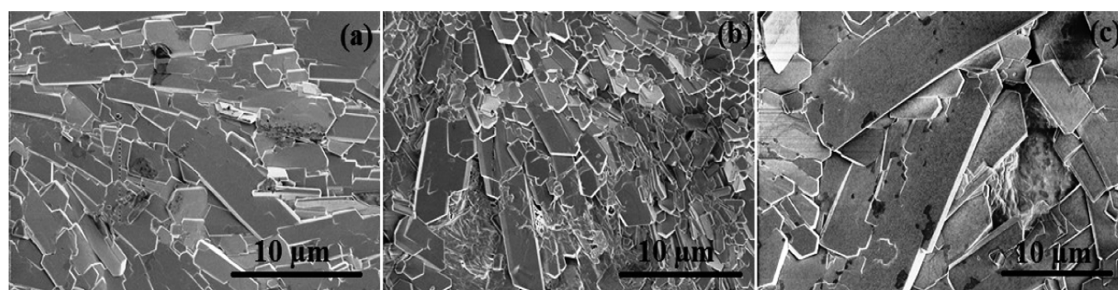
Figure 3. Scanning electron microscopy (SEM) images of (a) CMEG00, (b) CMEG25, and (c) CMEG50 showing platelet-like crystals (magnification level: 5000×).
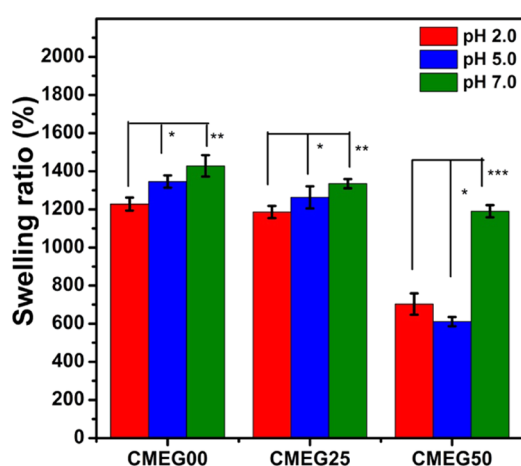
Figure 4. Swelling ratio of the films in Tris buffer of pHs 2.0, 5.0, and 7.0 at 37 °C after 12 h (*$p < 0.05$, **$p < 0.01$, ***$p < 0.001$, ns = not significant).

Table 2. Hemocompatibility Parameters of the Films Exposed to Blood[a]

parameters	control	CMEG00	CMEG25	CMEG50
WBC count %	5	11	8	31
RBC count %	5	3	1	13
platelets count %	10	6	5	12
hemolysis %	0.1	0.06	0.1	0.12
plasma hemoglobin (mg/dl)	4	8	13	16

[a]Empty polystyrene tube exposed to blood was taken as control.

metabolic activity cultivated in the medium exposed to the extracts as measured by thiazolyl blue tetrazolium blue (MTT) assay indicated appreciable cell proliferation for all films.

Effect of Films on Wound Healing. The aim of skin wound treatment is to restore and revive the structural and functional properties of damaged skin to normal tissue levels involving orchestrated regeneration of skin with accelerated neo-vascularization, angiogenesis, and scar-free integration of the surrounding skin. The efficacy of the films in wound healing under normal healthy and diabetic conditions was evaluated in rat models. Morphology of the gross appearance of the wounds

with and without films is shown in Figure 6 for different time periods (days 0, 8, and 16 postsurgery).

The wounds in normal healthy rats reduced significantly in size, whereas the size of diabetic wounds was not reduced to the same extent and the mean wound closure (%) calculated from the wound area is given in Figure 7. On day 8, the process of wound closure in normal rats was significantly facilitated by the films with mean wound closures of 70 ± 2, 60 ± 2, and 55 ± 2% compared to diabetic wounds with mean closures of 30 ± 1, 20 ± 3, and 20 ± 2% for CMEG00, CMEG25, and CMEG50, respectively ($p < 0.001$). In normal healthy wounds, the skin regeneration required 16 days to form complete skin, but wounds still persisted in the diabetic model at the same time point. The mean wound closures (%) of diabetic wounds were 60 ± 2, 50 ± 3, and 48 ± 3% on day 16 ($p < 0.001$) for different films. From this, it is evident that CMEG00 showed better wound healing in normal and diabetic wounds compared to blend film. For both the normal and diabetic control groups, after surgery, the unhealed area was higher and hair growth was comparatively slower than in the membrane-treated wounds. However, a significant difference between membrane-treated and -untreated was also noted. Normal wounds treated with membranes healed completely, whereas wound still persisted in the control.

Histopathological analysis provides the cellular and tissue-level interpretations of the wound healing process. The wound sections (days 8 and 12) stained with haemotoxylin and eosin (H&E) are shown in Figure 8. Generally, on day 8 postwounding, the wound exhibited inflammatory response and gradual granulation tissue formation and early collagen deposition. On day 12, granulation tissue formation with the onset of collagen remodeling was noted. In this study, on day 8 postsurgery, the untreated normal and diabetic wounds were characterized with inflammation along with the infiltration of neutrophils, whereas granulation tissue formation was noted for film-treated wounds in both the rat models. On day 12 postwounding, the formation of granulation tissues like fibroblasts was higher in the treated normal wound compared to the treated diabetic wounds. Inflammation still persisted in both the controls as represented by the presence of inflammation on day 12. Tissue formation is incomplete for both the control groups. The diabetic control group shows
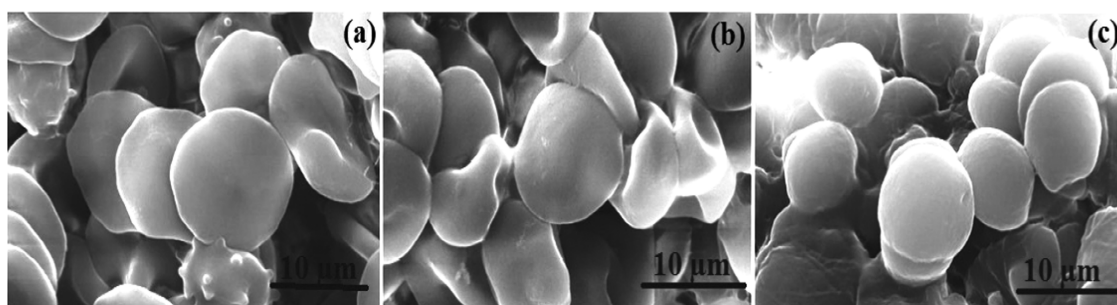
Figure 5. Scanning electron microscopy images of the red blood cells adhered to the films: (a) CMEG00; (b) CMEG25, and (c) CMEG50 after hemocompatibility test (magnification level: 15 000×).
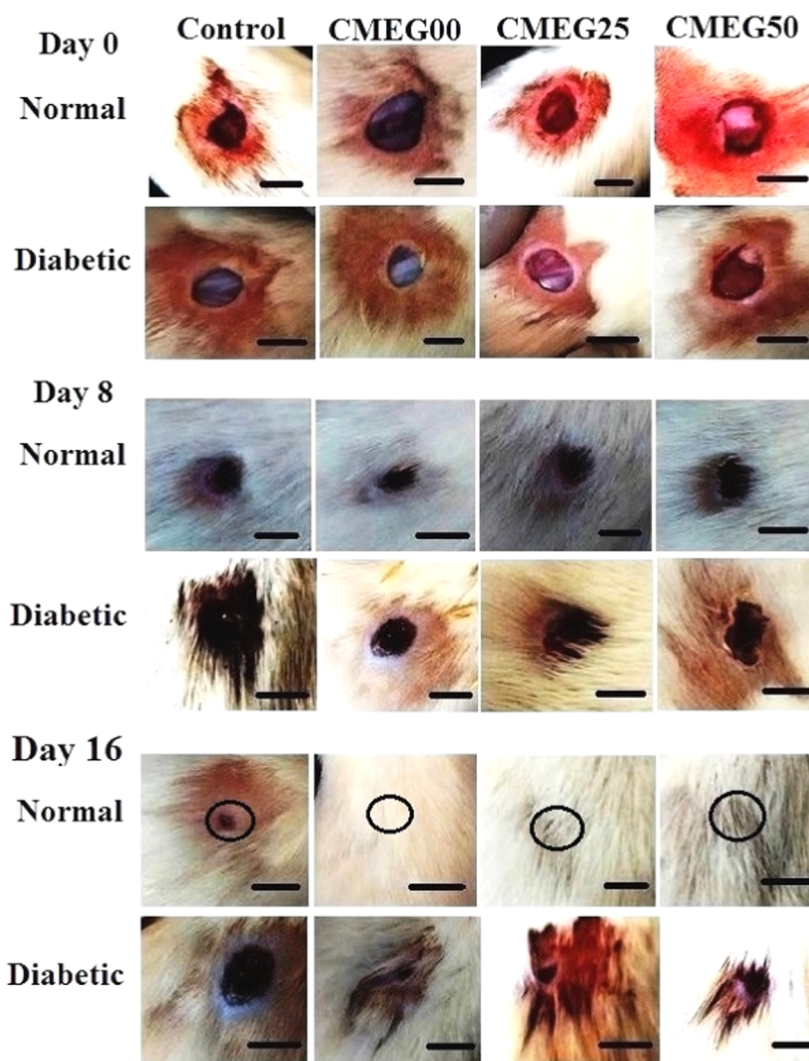

Figure 6. Photographs of the wound area in normal and diabetic rat models on days 0, 8, and 16 postsurgery, showing gradual healing of wound with time. The wound in normal healthy rat healed completely on 16th day (as marked by black circles), whereas in control and diabetic rats, the wound still persisted. The scale bar is 1 cm.

higher inflammation and necrosis compared to the normal control. The film-treated normal wound showed enhanced reepithelialization than diabetic wound.

The formation of collagen is a very crucial step in wound healing. Skin wound sections stained with Masson's trichrome to highlight the formation of collagen bundles are shown in Figure 9. Newly formed collagen fibers can be identified in film-treated normal and diabetic wounds compared to the control groups on day 8. Collagen deposition with a typical wavy pattern of collagen fibers was noted in normal wounds treated with films on day 12, whereas diabetic wounds exhibited lack of specific collagen fiber organization. Irregular collagen formation with incomplete tissue formation is noted for the control groups, and no improvement in wound healing is observed for the diabetic control. The diabetic control group shows the lowest rate of collagen synthesis and deposition. The
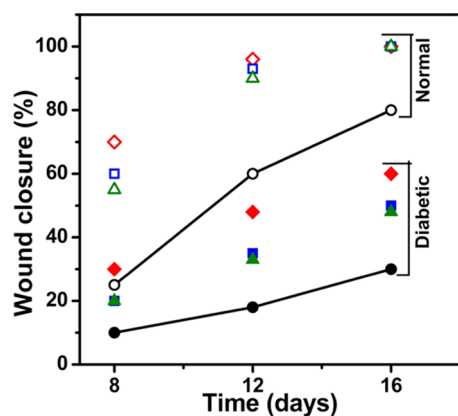
Figure 7. Percentage of wound closure in normal (unfilled symbols) and diabetic (filled symbols) rats on days 8, 12, and 16 compared individually. CMEG00, CMEG25, and CMEG50 films are represented as (◇), (□), and (△) respectively.

collagen deposition in film-treated groups is almost similar to the findings in normal skin, thus representing enhanced skin regeneration by the application of the films.[38] Overall, CMC-based films exhibit accelerated wound healing and more organized tissue formation and collagen deposition at the wound site than the blend films.

■ DISCUSSION

To fabricate an appropriate film for wound healing and skin regeneration applications, different crucial aspects are considered, including physicochemical, mechanical, morphological, and swelling properties, degradability, cell cytotoxicity, and finally, in vivo accommodation. Blending plays an important role in addressing the film structure pattern, mechanical strength, fluid absorption capability, and degradability. In this study, CMC and CMC/PEG blend films were prepared by solution casting method. CMC films were characterized by

XRD and FTIR to determine the structural phases and specific information about chemical bonding and molecular structure of CMC.

Thermal analyses, such as DSC and TGA, described the behavior of the films as a function of temperature and revealed the thermal transition, degradation process, and thermal stability of these films. The shapes of the thermograms for all of the films are identical; however, the endothermic peaks of the blend films became less prominent than that of the pure CMC films. The melting temperature depression for the blend films might be due to the presence of PEG in CMC, resulting in interaction between the functional groups of these two polymers.[39] All of the films exhibited steady degradation with the increase in heating temperature. The present study yielded low values of tensile properties of the films, although the tensile strength of skin is 1−100 MPa.[40] The seeding of cells may lead to strengthening of the films due to the secretion of extracellular matrix by the cells.[41]

Swelling ability has a prime significance in skin tissue engineering to enable films to respond to varying pHs and absorb wound exudate from the wound site. Healthy intact skin has acidic pH to regulate bacterial flora to prevent infection. The occurrence of wound disturbs the acidic milieu of skin, and the pH is disrupted, resulting in neutral pH of the tissue lying underneath the epidermis. The successful skin healing and reepithelialization help the skin to return to being acidic. Wound exhibits neutral pH during the healing process, which includes various factors like hypoxia and increased lactic acid formation. An acidic pH environment is desired to facilitate fibroblast proliferation, migration, and differentiation and also to prevent bacterial colonization. Delayed wound healing oscillates the pH, which becomes alkaline over time.[42] Thus, it is important to study the pH-responsive behavior of CMC in the physiological body fluid of different pHs (from acidic to neutral range).
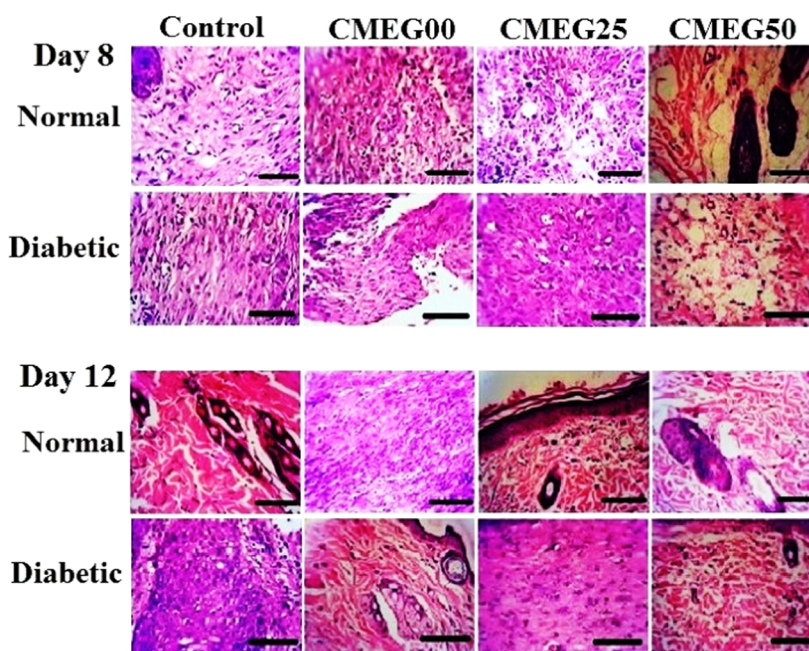

Figure 8. H&E staining of the wound sections collected on days 8 and 12 in normal and diabetic rat models. Control group is untreated open wounds, and experimental group is treated with three different films: CMEG00, CMEG25, and CMEG50.
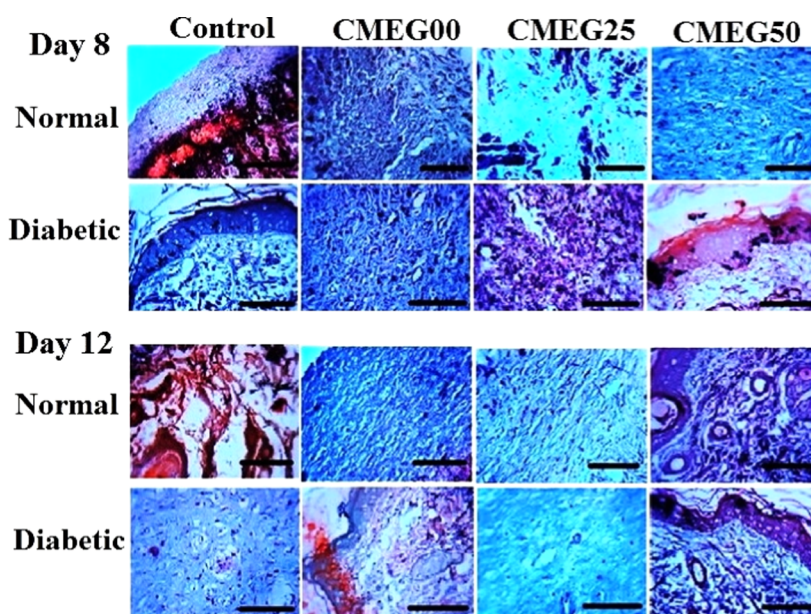
Figure 9. Masson's trichrome staining for histological sections on days 8 and 12 in normal and diabetic rat models. Original magnification 400× (the scale bar is 100 μm). Control group is untreated open wounds, and experimental group is treated with three different films: CMEG00, CMEG25, and CMEG50.

Swelling ability is affected when the films come in contact with external solution of different pHs. The effect of pH on swelling of the films was investigated in Tris buffer in acidic and neutral range of pH. The swelling ratio results showed that the films can serve as an excellent matrix to facilitate absorption of a huge amount of fluid. CMC films exhibited a higher swelling capability than the blends, and the swelling ability decreased with increase in PEG concentrations. The swelling ratio of the films was lower in acidic region (pHs 2.0 and 5.0) and was found to be higher at the neutral pH. These results can be correlated to the swelling ratio of pure CMC hydrogel with and without cross-linking, which showed a very small intake of fluid in a lower pH range and exhibited sufficient fluid uptake at higher pH. The uptake of water was pH-dependent, and the phenomenon is fully governed by protonated (COOH) hydrogen bond present in CMC. The polysaccharide chain without blend is not confined to any network, and COO$^-$ moieties (fixed negative charge) result in chain stiffening, thus initiating a large molecule of water absorption. CMC is an excellent adsorbent hydrogel, whose swelling behavior is notably influenced by the appreciable amount of CMC content in the films.[30] It is also noted that the swelling ratio of the films in Tris−HCL buffer increased from acidic region to the neutral region. The low swelling ability in acidic region can be due to COO$^-$ occupation of CMC by protonation in the buffer. This results in repulsive forces between carboxylate ions, thus resisting association with water through hydrogen bonding.[43] Generally, carboxylic group ionizes at higher pH, resulting in deprotonation. With the increase in pH of Tris buffer, the carboxylic group present in CMC ionizes, which generates anionic charged polymer chains due to self-repulsion of carboxylate ions, resulting in network chain expansion and leading to an increase in swelling.

Blood−material interaction is a key host reaction that occurs during implantation of a biomaterial. In this study, blood−material interaction was accounted by the deposition of blood cells and platelets on the prepared films. From wound healing perspective, deposition of blood cells on a biomaterial is defined as provisional matrix formation. Such matrix furnishes cellular components to initiate wound healing and reaction with foreign bodies. It directly influences and activates substances that are capable of macrophage activity modulation along with proliferation of cells in wound healing responses.[44] Hemocompatibility test is regarded as a simple, reliable, and effective method to measure material's hemostatic potentials. The interaction between cellular components and the films may lead to the damage of cells. These interactions can rupture the blood cells and the condition can be fatal; thus, blood−film interaction in terms of hemocompatibility test was conducted. The control sample showed 0.10% hemolysis. Generally, a biomaterial should yield at least 2% hemolysis.[45] The hemolytic potentials of CMEG00, CMEG25, and CMEG50 are 0.06, 0.10, and 0.12% and the values are <0.14%, which exhibited negligible hemolytic property according to American Society for Testing and Materials (ASTM F756-00, 2000). In addition, the cell viability results indicated that the fibroblast cells were viable and proliferated normally in the presence of film extracts, thus confirming film benefits for cell growth.

The efficiency of the films to treat full-thickness normal and diabetic wounds in rats was also evaluated. The wound healing process can be classified into three overlapping stages: inflammation, proliferation, and tissue regeneration. The films were not removed from the wound site during in vivo experiment. The films were expected to degrade at the wounded region, which is also an important factor in influencing new tissue formation.[46] The application of films on the wound site increased the wound healing rate. The wound was smaller and the reepithelialization propensity was higher in rats treated with pure CMC films than the blends and the control. A study by Lee et al. indicated that the acceleration of open full-thickness wound healing is observed with layered chitosan-based hydrogel treatment, which occurred in 21 days.[47] Findings on wound healing efficacy of CMC scaffolds suggested that these scaffolds demonstrated reduction in partial-thickness wound size and gained full reepithelialization in 22 days.[48] The prepared films required shorter duration to

achieve complete reepithelialization of the normal as well as diabetic wounds. The speedy recovery of wound can be due to the presence of CMC polymer in the films. CMC might have favored neutrophil accumulation at the wound site without inducing further inflammation. These results can be correlated to the one-step procedure application of meshed autograft/commercially available Integra, silver nylon, Biobrane and Vaseline gauzes in facilitating wound closure within 6−19 days in rat model and also macroporous waterborne polyurethane/chitosan hydrogel scaffolds, which required 21 days for complete wound recovery in rat model.[49,50]

The most common histopathology methods, H&E and Masson's trichrome staining, were used to assess the formation of granulation tissue and collagen during the wound healing process. The histopathological analysis revealed that the neutrophils infiltrated at the site of the skin wound. Accumulation of excess neutrophils had a direct influence on the reduction of wound closure rate.[51] When the neutrophil inflammation declines, macrophages approach toward the wound site and refill the wound. At the same time, the epidermis surrounding the edges of the wound allows epithelial cell migration, resulting in the onset of reepithelialization.[52] The major role of epidermis is to prevent loss of water and to minimize the exposure to potential bacterial infection.[53] Generally, full-thickness skin wound is difficult to heal and is characterized by scar even after complete healing. On the other hand, complete diabetic wound closure is difficult to achieve as such healing process is very complex and involves changes in vascularization, immune and biomechanical functions, and neuropathy.[54,55] Thus, appropriate material is highly desirable to meet the need of rapid wound closure by promoting wound healing and scar reduction. The wound covering by the films decreased hemorrhage and exudation at the wound site. In the middle stage, granulation tissues containing fibroblasts and new capillaries formation were observed in all of the film-treated normal and diabetic wounds, which were not prominent in the control groups. In the later stage, collagen fiber formation is observed, which further accelerated the wound healing process. The collagen deposition in film-treated normal wounds was found to be more organized than that in film-treated diabetic wounds. Application of films at the wound site did not interrupt the process of wound healing, instead, potentially accelerated healing by inhibiting neutrophil infiltration and promoting reepithelialization. These results agree with the results obtained by utilizing one of the most important polymers used for wound healing, i.e., chitosan. Chitosan fosters sufficient granulation tissue formation accompanied by deposition of thin collagen fibers. The prepared films showed similar results like chitosan dressings. CMC-based films kept the wounds moist and also encouraged granulation tissue growth and reduced the formation of scar. The films contain polysaccharide chain, which promotes wound healing by providing moist environment around the wound, favoring tissue granulation to achieve hemostasis. CMC films might absorb wound fluid by ion exchange. This can promote granulation tissue formation, rapid epithelialization, as well as healing, resulting in increase of healing time and quality with polysaccharide-based films. It can be assumed that the faster wound healing with the films is nearly related to polymer degradation at the wound site, which could stimulate aggregation of inflammatory cells and promote migration of epithelial, vascular endothelial, and fibroblast cells, leading to a significantly higher and accelerated wound healing of films

than the control groups. The systemic histopathological analysis provided evidence directly to improve the understandings of the efficacy of the CMC-based films, thus encouraging further research and utility of such films.

Thus, the prepared films can be considered as potential biomaterials due to their crystalline morphology, high swelling capability, biodegradability, good cytocompatibility, and fibroblast and collagen production characteristics. Generally, natural polymers like chitosan, collagen, and gelatin are often cross-linked or blended with PVA, PEG, and PCL to improve the various characteristic properties of the materials. In this study, it is also evident that pure CMC films exhibit enhanced properties in all terms than the blends, which suggests the potential of CMC to be used alone without any additives or cross-linkers as a unique polymer matrix for critical chronic wound healing applications.

■ CONCLUSIONS

In the present study, CMC and CMC/PEG blend films were prepared by solution-casting method as wound dressings. The films were characterized by different techniques to establish them as suitable templates as wound healing materials. The XRD and FTIR analyses confirmed the purity of CMC in the films and showed the crystalline property of CMC. The films are pH-responsive and exhibit low to high swelling ratio over a considerable range of pH (2.0, 5.0, and 7.0). The films are found to be hemocompatible with less than 2% hemolysis. These films are noncytotoxic and support fibroblast cell proliferation. The wound healing process using normal and diabetic rats indicated that pure CMC films are more effective in healing wounds than the blends, but all of the films have the capability to accelerate the wound healing process. The histopathological study showed that the films can promote reepithelialization by the formation of granulation tissue and collagen synthesis at the wound site. Overall, the prepared films can serve as an excellent template for successful tissue regeneration in skin tissue engineering application.

■ EXPERIMENTAL SECTION

Materials. Sodium carboxymethyl cellulose (CMC) (viscosity: 250−450 cps), poly(ethylene glycol) (PEG) (MW, 4000 Da), phosphate-buffered saline (PBS) powder, Tris buffer powder, hydrochloric acid, streptozotocin, sodium citrate, hematoxylin, and eosin (2% w/v) were purchased from HiMedia, India. Dulbecco's modified Eagle's medium (DMEM), thiazolyl blue tetrazolium blue (MTT), dimethyl sulfoxide, and Masson's trichrome stain kit were obtained from Sigma-Aldrich, Germany. Penicillin and streptomycin were received from Biochrom AG, Germany.

Preparation of Films. CMC and CMC/PEG blend films were prepared by solution casting method. CMC solution (2.5 wt %) and different concentrations of PEG (0.025% and 0.05% w/v) were mixed to form a polymer blend. The polymer blend solutions were homogenized at room temperature for 30 min and filtered to remove the air bubbles trapped inside the viscous solutions. The solutions were cast in a mold and transferred into an hot-air oven preset at a temperature of 40 °C. After 72 h of complete drying, the films were removed and stored in a desiccator. The films are named as CMEG00, CMEG25, and CMEG50, where the last two digits indicate the amount of PEG used.

Characterization of the films. *X-ray Diffraction (XRD).* XRD study was done using an X-ray diffractometer (GE Inspection, XRD 3003TT, Germany) to examine the crystalline nature of films, with a monochromatic Cu Kα (λ = 1.54 A°) The X-ray source was operated at 40 kV, scanned in the 2θ range of 10−70° with a step size of 0.02/s.

Fourier Transform Infrared (FTIR) Spectroscopy. The chemical compositions of the films were characterized using a Fourier transform infrared spectrophotometer (IRA Shimadzu, Japan) equipped with ZnSe cell/crystals by identifying the functional groups of CMC and PEG. All of the spectra were recorded within a range of 4000−400 cm^{-1} with a resolution of 4 cm^{-1}.

Thermal Characterization. The glass-transition or crystal-line temperature of the polymer blends was determined using a differential scanning calorimeter (DSC 204 Netzsch, Germany) from 25 to 500 °C at a scanning rate of 10 K/min under nitrogen atmosphere. The thermal properties of the films were analyzed by a thermogravimetric analyzer (TGA, Q50V20.13 Build 39, TA Instruments) from 25 to 800 °C at a constant heating rate of 10 K/min under a constant flowing nitrogen atmosphere.

Tensile Test. The mechanical properties of the films were determined at room temperature using Texture Analyzer (CT V1.4 Build 17, Brookfield Engineering Labs, Inc.) under tensile mode. Specimens of 50 × 5 mm size were applied with a trigger load of 5 g using a load cell of 10 kg and a cross-head speed of 0.1 mm/s. The maximum stress, tensile strength, and Young's modulus were evaluated from the stress−strain data at breaking yield point.

Scanning Electron Microscopy (SEM). The surface morphology of the films was examined using a scanning electron microscope (Carl Zeiss, EVO 18 SEM, Germany) operated at 30 kV and at a working distance of 6 mm. All of the films were coated with gold for 10 min under high vacuum at 20 kV using a sputter coater (Cressington Sputter Coater, 108auto).

Effect of pH on Swelling Property. To study the effect of pH on films swelling, the films were immersed in Tris−HCL buffer (pHs 2.0, 5.0, and 7.0) at 37 °C for 12 h and the swelling ratio (SR) was calculated using eq 1. The experiment was carried out in triplicate.

$$SR\ (\%) = \frac{w_t - w_i}{w_i} \times 100 \tag{1}$$

where w_i is the initial weight of the films in the dry state and w_t is the weight of the swollen films.

Biological Characterization. *Hemocompatibility Test.* Hemocompatibility test was performed to evaluate the interaction of blood cells with the films. Whole blood was stored in polystyrene tubes preloaded with anticoagulant, citrate phosphate, and dextrose solution to optimize the storage condition of the blood cells. About 3 mL of anticoagulated blood was introduced into the 10 mL polystyrene tubes containing the films. Then, 1 mL of blood was taken out immediately from the tubes for blood cell count. Percentage of hemolysis and plasma hemoglobin was measured by agitating the remaining blood in contact with the films in an incubator for 30 min at 75 rpm in an environmental shaker thermostated at 37 °C. Empty polystyrene tube exposed to blood was taken as control. The experiment was performed in triplicate.

After 24 h, the films in contact with blood were sterilized in ethanol solution for 30 min and rinsed thoroughly with PBS (pH 7.4). The films were dried and then incubated at 37 °C for 4 h to adhere and fixed with 2.5% glutaraldehyde and analyzed using a scanning electron microscope.

Cytotoxicity Test. The cytotoxicity of the films was evaluated by indirect dilution method by preparing extracts of the films in DMEM and by treating with fibroblast cells (NIH 3T3) via cell viability and MTT assays. Initially, the cells were maintained in DMEM supplemented with 10% fetal bovine serum, 100 units/mL penicillin, and 100 units/mL streptomycin at 37 °C in a 5% CO_2 atmosphere. The cells were added to the extracts at a density of $1 \times 10^5/500$ μL culture medium in each well in a 24-well plate and incubated for 3 days to determine the cell viability quantitatively using a cell viability autoanalyzer (Vi-CELL XR, Beckman Coulter). For MTT assay, the MTT solution diluted with PBS was added to the cell medium and incubated for 4 h at 37 °C in a 96-well plate. The unreacted MTT solution was removed and dimethyl sulfoxide was introduced to dissolve the accumulated formazan crystal giving a purple solution. The absorbance of the colored solution was measured at 570 nm using Elisa Microplate Reader (Multiscan Ex, Thermo Scientific) in terms of cell viability (%).

In Vivo Full-Thickness Wound Healing Study. To evaluate the efficiency of the films for wound healing, full-thickness wounds were created in male Wistar albino normal and diabetic rats. All of the animal procedures were carried out in compliance with the experimental protocols approved by Institute Animal Ethics Committee (IAEC) of Chettinad Hospital and Research Institute (CHRI), Chennai, India. Diabetes was induced in rats using a single dose of intraperitoneal injection of 60 mg/kg streptozotocin dissolved in saline-sodium citrate buffer (0.1 M, pH 4.5). The blood glucose level was monitored using a blood glucose monitor (Accu-Check) at regular time periods. The rats showing blood glucose level >200 mg/dL were considered diabetic. Diabetes was maintained in rats throughout the experiment by feeding glucose to them.

For surgical procedure, the animals were anesthetized with halothane, placed in prone position, and the hair from the dorsal region was shaved using a razor blade. A circular full-thickness wound (1 cm diameter) was created on the dorsum of each rat. The wounds in normal healthy and diabetic wounds were treated with CMEG00, CMEG25, and CMEG50 and compared to the untreated group. The films were applied only once and wound closure was measured at specific time points. All measures were taken to minimize pain during the surgical procedures, and at the end of the study, the rats were euthanized by halothane inhalation to collect the skin at closed wounds for histopathological analysis.

Macroscopic Evaluation of Wound Healing. The surface of the wound area was photographed using a digital camera (Nikon Coolpix A10) on the day of wound incision, days 0, 8, and 16, and the wound size profile in terms of wound closure (%) was calculated by the equation.

$$\begin{aligned} &\text{wound closure (\%)} \\ &= \frac{(\text{area of the actual wound} - \text{area of the unhealed wound})}{\text{area of the actual wound}} \times 100 \end{aligned}$$

Histopathology. For histological analysis, the wounds were excised from rats after euthanizing them on days 8 and 12 and fixed in 10% formaldehyde solution. After fixation, the

specimens were dehydrated in ethanol and embedded in paraffin. The specimens were sectioned at 4 μm using microtome and stained with hematoxylin–eosin (H&E) for the assessment of cell morphology and proliferation, and with Masson's trichrome stain to visualize collagen matrix formation at the wound site.

Statistical Analysis. The experimental data for maximum stress, Young's modulus, ultimate tensile strength, and swelling ratio are reported as mean ± SD and analyzed by one-way ANOVA, followed by Tukey's post-test for attaining statistical significance. GraphPad Prism v5.01 was used to find statistical significance, and $p < 0.05$ was considered statistically significant.

■ AUTHOR INFORMATION

Corresponding Author
*E-mail: i.manjubala@vit.ac.in.

ORCID ●

Inderchand Manjubala: 0000-0003-4873-2377

Author Contributions
I.M. formulated the concept, idea, and methodology; analyzed the data; and discussed and contributed for framing and writing the manuscript. The experiments were performed by P.B. The animal experiments were conducted and supervised by Dr R.A. and Dr S.D. The results were analyzed, discussed, and manuscript framing was done by Dr U.N. The manuscript was written through contributions of all authors. All authors have given approval to the final version of the manuscript.

Notes
The authors declare no competing financial interest.

■ ACKNOWLEDGMENTS

■ REFERENCES

(1) Sood, A.; Granick, M. S.; Tomaselli, N. L. Wound dressings and comparative effectiveness data. *Adv. Wound Care* **2014**, *3*, 511–529.

(2) Dhivya, S.; Padma, V. V.; Santhini, E. Wound dressings—a review. *BioMedicine* **2015**, *5*, 22.

(3) Ovington, L. G. Advances in wound dressings. *Clin. Dermatol.* **2007**, *25*, 33–38.

(4) Asti, A.; Gioglio, L. Natural and synthetic biodegradable polymers: different scaffolds for cell expansion and tissue formation. *Int. J. Artif. Organs* **2014**, *37*, 187–205.

(5) Moura, L. I. F.; Dias, A. M. A.; Carvalho, E.; de Sousa, H. C. Recent advances on the development of wound dressings for diabetic foot ulcer treatment—A review. *Acta Biomater.* **2013**, *9*, 7093–7114.

(6) Basu, P.; NarendraKumar, U.; Manjubala, I. Wound healing materials-a perspective for skin tissue engineering. *Curr. Sci.* **2017**, *112*, 2392–2404.

(7) Natarajan, V.; Krithica, N.; Madhan, B.; Sehgal, P. K. Preparation and properties of tannic acid cross-linked collagen scaffold and its application in wound healing. *J. Biomed. Mater. Res., Part B* **2013**, *101*, 560–567.

(8) Tseng, H. J.; Tsou, T. L.; Wang, H. J.; Hsu, S. H. Characterization of chitosan-gelatin scaffolds for dermal tissue engineering. *J. Tissue Eng. Regener. Med.* **2013**, *7*, 20–31.

(9) Wang, X.; You, C.; Hu, X.; Zheng, Y.; Li, Q.; Feng, Z.; Sun, H.; Gao, C.; Han, C. The roles of knitted mesh-reinforced collagen-chitosan hybrid scaffold in the one-step repair of full-thickness skin defects in rats. *Acta Biomater.* **2013**, *9*, 7822–7832.

(10) Li, H.; Xue, Y.; Jia, B.; Bai, Y.; Zuo, Y.; Wang, S.; Zhao, Y.; Yang, W.; Tang, H. The preparation of hyaluronic acid grafted pullulan polymers and their use in the formation of novel biocompatible wound healing film. *Carbohydr. Polym.* **2018**, *188*, 92.

(11) Waghmare, V. S.; Wadke, P. R.; Dyawanapelly, S.; Deshpande, A.; Jain, R.; Dandekar, P. Starch based nanofibrous scaffolds for wound healing applications. *Bioact. Mater.* **2018**, *3*, 255–266.

(12) Berce, C.; Muresan, M. S.; Soritau, O.; Petrushev, B.; Tefas, L.; Rigo, I.; Ungureanu, G.; Catoi, C.; Irimie, A.; Tomuleasa, C. Cutaneous wound healing using polymeric surgical dressings based on chitosan, sodium hyaluronate and resveratrol. A preclinical experimental study. *Colloids Surf., B* **2018**, *163*, 155–166.

(13) Xie, H.; Chen, X.; et al. Preparation of chitosan-collagen-alginate composite dressing and its promoting effects on wound healing. *Int. J. Biol. Macromol.* **2018**, *107*, 93–104.

(14) Zhong, S. P.; Zhang, Y. Z.; Lim, C. T. Tissue scaffolds for skin wound healing and dermal reconstruction. Wiley interdisciplinary reviews. *Wiley Interdisc. Rev.: Nanomed. Nanobiotechnol.* **2010**, *2*, 510–525.

(15) Mano, J. F.; Silva, G.; Azevedo, H. S.; Malafaya, P.; Sousa, R.; Silva, S.; Boesel, L.; Oliveira, J. M.; Santos, T.; Marques, A. Natural origin biodegradable systems in tissue engineering and regenerative medicine: present status and some moving trends. *J. R. Soc., Interface* **2007**, *4*, 999–1030.

(16) Shanmugasundaram, O. L.; Syed Zameer Ahmed, K.; Sujatha, K.; Ponnmurugan, P.; Srivastava, A.; Ramesh, R.; Sukumar, R.; Elanithi, K. Fabrication and characterization of chicken feather keratin/polysaccharides blended polymer coated nonwoven dressing materials for wound healing applications. *Mater. Sci. Eng., Proc. Conf.* **2018**, *92*, 26–33.

(17) Fan, L.; Yang, H.; Yang, J.; Peng, M.; Hu, J. Preparation and characterization of chitosan/gelatin/PVA hydrogel for wound dressings. *Carbohydr. Polym.* **2016**, *146*, 427–434.

(18) Kakkar, P.; Verma, S.; Manjubala, I.; Madhan, B. Development of keratin–chitosan–gelatin composite scaffold for soft tissue engineering. *Mater. Sci. Eng., Proc. Conf.* **2014**, *45*, 343–347.

(19) Mogoşanu, G. D.; Grumezescu, A. M. Natural and synthetic polymers for wounds and burns dressing. *Int. J. Pharm.* **2014**, *463*, 127–136.

(20) Vasconcelos, A.; Gomes, A. C.; Cavaco-Paulo, A. Novel silk fibroin/elastin wound dressings. *Acta Biomater.* **2012**, *8*, 3049–3060.

(21) Vepari, C.; Kaplan, D. L. Silk as a Biomaterial. *Prog. Polym. Sci.* **2007**, *32*, 991–1007.

(22) Aramwit, P.; Towiwat, P.; Srichana, T. Anti-inflammatory potential of silk sericin. *Nat. Prod. Commun.* **2013**, *8*, 501–504.

(23) Ehterami, A.; Salehi, M.; Farzamfar, S.; Vaez, A.; Samadian, H.; Sahrapeyma, H.; Mirzaii, M.; Ghorbani, S.; Goodarzi, A. In vitro and in vivo study of PCL/COLL wound dressing loaded with insulin-chitosan nanoparticles on cutaneous wound healing in rats model. *Int. J. Biol. Macromol.* **2018**, *117*, 601–609.

(24) Gutha, Y.; Pathak, J. L.; Zhang, W.; Zhang, Y.; Jiao, X. Antibacterial and wound healing properties of chitosan/poly(vinyl alcohol)/zinc oxide beads (CS/PVA/ZnO). *Int. J. Biol. Macromol.* **2017**, *103*, 234–241.

(25) Nair, L. S.; Laurencin, C. T. Biodegradable polymers as biomaterials. *Prog. Polym. Sci.* **2007**, *32*, 762−798.

(26) Boateng, J. S.; Matthews, K. H.; Stevens, H. N.; Eccleston, G. M. Wound healing dressings and drug delivery systems: a review. *J. Pharm. Sci.* **2008**, *97*, 2892−2923.

(27) Bhardwaj, N.; Chouhan, D.; Mandal, B. B. Tissue Engineered Skin and Wound Healing: Current Strategies and Future Directions. *Curr. Pharm. Des.* **2017**, *23*, 3455−3482.

(28) Hebeish, A.; Hashem, M.; El-Hady, M. M. A.; Sharaf, S. Development of CMC hydrogels loaded with silver nano-particles for medical applications. *Carbohydr. Polym.* **2013**, *92*, 407−41.

(29) Basu, P.; Repanas, A.; Chatterjee, A.; Glasmacher, B.; NarendraKumar, U.; Manjubala, I. PEO−CMC blend nanofibers fabrication by electrospinning for soft tissue engineering applications. *Mater. Lett.* **2017**, *195*, 10−13.

(30) Barbucci, R.; Magnani, A.; Consumi, M. Swelling behavior of carboxymethylcellulose hydrogels in relation to cross-linking, pH, and charge density. *Macromolecules* **2000**, *33*, 7475−7480.

(31) Ludwig, A. The use of mucoadhesive polymers in ocular drug delivery. *Adv. Drug Delivery Rev.* **2005**, *57*, 1595−1639.

(32) Zakharov, N.; Ezhova, Z. A.; Koval', E.; Kalinnikov, V.; Chalykh, A. Hydroxyapatite-carboxymethyl cellulose nanocomposite biomaterial. *Inorg. Mater.* **2005**, *41*, 509−515.

(33) Ng, S.-F.; Jumaat, N. Carboxymethyl cellulose wafers containing antimicrobials: A modern drug delivery system for wound infections. *Eur. J. Pharm. Sci.* **2014**, *51*, 173−179.

(34) Cheng, G.; Wang, T.; Zhao, Q.; Ma, X.; Zhang, L. Preparation of cellulose acetate butyrate and poly(ethylene glycol) copolymer to blend with poly(3-hydroxybutyrate). *J. Appl. Polym. Sci.* **2006**, *100*, 1471−1478.

(35) Qi, X.-M.; Liu, S.-Y.; Chu, F.-B.; Pang, S.; Liang, Y.-R.; Guan, Y.; Peng, F.; Sun, R.-C. Preparation and characterization of blended films from quaternized hemicelluloses and carboxymethyl cellulose. *Materials* **2015**, *9*, 4−16.

(36) El-Sayed, S.; Mahmoud, K.; Fatah, A.; Hassen, A. DSC, TGA and dielectric properties of carboxymethyl cellulose/polyvinyl alcohol blends. *Phys. B* **2011**, *406*, 4068−4076.

(37) Garai, S.; Sinha, A. Biomimetic nanocomposites of carboxymethyl cellulose−hydroxyapatite: novel three dimensional load bearing bone grafts. *Colloids Surf., B* **2014**, *115*, 182−190.

(38) Groeber, F.; Holeiter, M.; Hampel, M.; Hinderer, S.; Schenke-Layland, K. Skin tissue engineering—in vivo and in vitro applications. *Adv. Drug Delivery Rev.* **2011**, *63*, 352−366.

(39) Gupta, B.; Agarwal, R.; Alam, S. Preparation and characterization of polyvinyl alcohol-polyethylene oxide-carboxymethyl cellulose blend membranes. *J. Appl. Polym. Sci.* **2013**, *127*, 1301−1308.

(40) Hussain, S.; Limthongkul, B.; Humphreys, T. The Biomechanical Properties of the Skin. Dermatol Surg.2013, 39, 193-203. The Biomechanical Properties of the Skin. *Dermatol. Surg.* **2013**, *39*, 193−203.

(41) Karadas, O.; Yucel, D.; Kenar, H.; Torun Kose, G.; Hasirci, V. Collagen scaffolds with in situ-grown calcium phosphate for osteogenic differentiation of Wharton's jelly and menstrual blood stem cells. *J. Tissue Eng. Regener. Med.* **2014**, *8*, 534−545.

(42) Jones, E. M.; Cochrane, C. A.; Percival, S. L. The Effect of pH on the Extracellular Matrix and Biofilms. *Adv. Wound Care* **2015**, *4*, 431−439.

(43) Wei, Q.-B.; Luo, Y.-L.; fu, F.; Zhang, Y. Q.; Ma, R. X. Synthesis, characterization, and swelling kinetics of pH-responsive and temperature-responsive carboxymethyl chitosan/polyacrylamide hydrogels. *J. Appl. Polym. Sci.* **2013**, *129*, 806−814.

(44) Xu, F.; Nacker, J. C.; Crone, W. C.; Masters, K. S. The haemocompatibility of polyurethane−hyaluronic acid copolymers. *Biomaterials* **2008**, 150−160.

(45) Kuo, K.-C.; Lin, R.-Z.; Tien, H.-W.; Wu, P.-Y.; Li, Y.-C.; Melero-Martin, J. M.; Chen, Y.-C. Bioengineering vascularized tissue constructs using an injectable cell-laden enzymatically crosslinked collagen hydrogel derived from dermal extracellular matrix. *Acta Biomater.* **2015**, *27*, 151−166.

(46) Zhao, X.; Wu, H.; Guo, B.; Dong, R.; Qiu, Y.; Ma, P. X. Antibacterial anti-oxidant electroactive injectable hydrogel as self-healing wound dressing with hemostasis and adhesiveness for cutaneous wound healing. *Biomaterials* **2017**, *122*, 34−47.

(47) Lee, Y.-H.; Chang, J.-J.; Yang, M.-C.; Chien, C.-T.; Lai, W.-F. Acceleration of wound healing in diabetic rats by layered hydrogel dressing. *Carbohydr. Polym.* **2012**, *88*, 809−819.

(48) Ramli, N. A.; Wong, T. W. Sodium carboxymethylcellulose scaffolds and their physicochemical effects on partial thickness wound healing. *Int. J. Pharm.* **2011**, *403*, 73−82.

(49) Chu, C.-S.; McManus, A. T.; Matylevich, N. P.; Goodwin, C. W.; Pruitt, B. A., Jr. Integra as a dermal replacement in a meshed composite skin graft in a rat model: a one-step operative procedure. *J. Trauma Acute Care Surg.* **2002**, *52*, 122−129.

(50) Bankoti, K.; Rameshbabu, A. P.; Datta, S.; Maity, P. P.; Goswami, P.; Datta, P.; Ghosh, S. K.; Mitra, A.; Dhara, S. Accelerated healing of full thickness dermal wounds by macroporous waterborne polyurethane-chitosan hydrogel scaffolds. *Mater. Sci. Eng., Proc. Conf.* **2017**, *81*, 133−143.

(51) Kondo, T. Timing of skin wounds. *Leg. Med.* **2007**, *9*, 109−114.

(52) Park, J. E.; Barbul, A. Understanding the role of immune regulation in wound healing. *Am. J. Surg.* **2004**, *187*, S11−S16.

(53) Tsirogianni, A. K.; Moutsopoulos, N. M.; Moutsopoulos, H. M. Wound healing: Immunological aspects. *Injury* **2006**, *37*, S5−S12.

(54) Shen, Y.-I.; Cho, H.; Papa, A. E.; Burke, J. A.; Chan, X. Y.; Duh, E. J.; Gerecht, S. Engineered human vascularized constructs accelerate diabetic wound healing. *Biomaterials* **2016**, *102*, 107−119.

(55) Wang, W.; Lin, S.; Xiao, Y.; Huang, Y.; Tan, Y.; Cai, L.; Li, X. Acceleration of diabetic wound healing with chitosan-crosslinked collagen sponge containing recombinant human acidic fibroblast growth factor in healing-impaired STZ diabetic rats. *Life Sci.* **2008**, *82*, 190−204.